Journal of Hazardous Materials 185 (2011) 1273–1279

Contents lists available at ScienceDirect

Journal of Hazardous Materials

journal homepage: www.elsevier.com/locate/jhazmat

Modeling of nonylphenol degradation by photo-nanocatalytic process via multivariate approach

A.A. Babaei[a,b], A.R. Mesdaghiniai[a], N. Jaafarzadeh Haghighi[b], R. Nabizadeh[a], A.H. Mahvi[a,*]

[a] Department of Environmental Health Engineering and Center for Environmental Research, School of Public Health, Tehran University of Medical Sciences, Tehran, Iran
[b] Department of Environmental Health, School of Public Health, Ahvaz Jundishapur University of Medical Sciences, Ahvaz, Iran

ARTICLE INFO

Article history:
Received 20 April 2010
Received in revised form 4 September 2010
Accepted 11 October 2010
Available online 16 October 2010

Keywords:
Nonylphenol
Photo-nanocatalysis
Modeling
Factorial design
Multivariate approach
RSM plots

ABSTRACT

Modeling of photocatalytic degradation of nonylphenol (NP), an endocrine disrupter and toxic compound, has been investigated in synthetic aqueous solutions containing ZnO nanoparticles as semiconductor using multivariate approach. In this regard, a full factorial experimental design was performed in order to study the main variables affecting the degradation process as well as their most significant interactions. Initial NP concentrations ($[NP]_0$) of 0.454–9.08 μM, were treated with UV–vis/ZnO using different pH and nanocatalyst loading rates. Effect of experimental parameters on the NP degradation rate constant was established by the response surface plots. The degradation rate constant decreased with an increase in the initial concentration of NP, while it increased with ZnO loading until a concentration of 0.5 g L^{-1}. The rate constant increases with increase in pH up to 10, after which a significant decrease is observed.

The results showed that most influential factors on NP degradation constant are the $[NP]_0$, pH of reaction media, and ZnO loading rate, and the most significant interaction is [NP]-pH. Finally, two mathematical models have been proposed to estimate NP degradation rate constant (k) on the basis of the significant variables and interactions. Predicted results of models showed good agreement with the experimental data (R^2 = 0.83 and 0.93).

1. Introduction

During biological wastewater treatment nonylphenol polyethoxylates (NPnEOs) which they are common non-ionic surfactants partially converted to more persistent and toxic metabolite nonylphenol (NP) [1–4]. Additionally, NP is a raw material for the production of NPnEOs as well as other chemicals such as phosphate antioxidants, modified phenolic resins, additives to machine oils and metallurgical oils [1]. NP, which has numerous isomers, is an endocrine disrupter, toxic to aquatic organisms and xenobiotic compound from sewage disposal plants, show estrogenic activities at very low concentrations (ppb level), and their feminizing effect on fish is a serious problem in terms of ecological system conservancy [5,6]. Currently the EPA has accepted the risks of nonylphenol and has prepared a guideline for ambient water quality that recommends nonylphenol concentrations in freshwater be below 6.6 μg L^{-1} and, in saltwater, below 1.7 μg L^{-1} [7].

Due to its refractory and toxic nature, and the relatively low efficiency of the current remediation process, the advanced oxidation processes (AOPs), based on the generation of highly reactive species such as hydroxyl radicals (•OH), appear to be a promising alternative for the removal of such a substance. Among different AOPs, photocatalysis processes have been widely used for different treatment purposes.

Recently, removal of aqueous NPs by electrochemical [8], ozonation [8–12], photolysis with UV [13], Photocatalysis with UV/TiO_2 and UV/$BiVO_4$ [12,14–16], and Sonolysis with Fe(II) and Fe(III) [17] has been reported.

However, photocatalysis with UV/ZnO, one of the most promising advanced oxidation processes for the destruction of aquatic pollutants, has not been reported for the degradation of NPs. One of the most important aspects of environmental photocatalysis is the selection of semiconductor materials such as ZnO and TiO_2: two ideal photocatalysts in several respects. For example, they are relatively inexpensive, and they provide photogenerated holes with high oxidizing power due to their wide band gap energy. Since ZnO has nealrly the same band gap energy (3.2 eV) as TiO_2, its photocatalytic capacity is anticipated to be similar to that of TiO_2. The greatest preference of ZnO in comparison with TiO_2 is that it absorbs over a larger fraction of the UV spectrum and the corresponding threshold of ZnO is 425 nm [18]. For this reason, ZnO photocatalyst is the most suitable for photocatalytic degradation in the presence of sunlight.

Reaction mechanisms of photocatalytic processes have been discussed extensively in the literature [19,20]. Briefly, illumination of

* Corresponding author. Tel.: +98 2188954914; fax: +98 2166462267.
E-mail address: ahmahvi@yahoo.com (A.H. Mahvi).

0304-3894/$ – see front matter © 2010 Elsevier B.V. All rights reserved.
doi:10.1016/j.jhazmat.2010.10.042

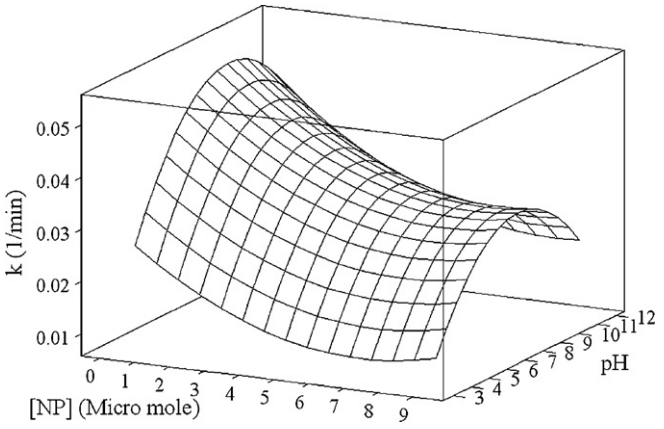

Fig. 1. The response surface plot of the NP degradation rate constant as the function of initial NP concentration (μM) and medium pH.

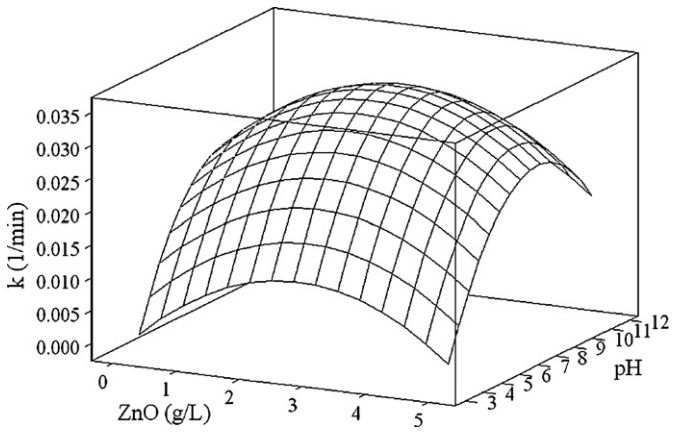

Fig. 3. The response surface plot of the NP degradation rate constant as the function of medium pH and ZnO loading rate ($g\,L^{-1}$).

aqueous ZnO suspension with irradiation energy greater than the band gap energy (E_{bg}) of the semiconductor ($h\nu > E_{bg} = 3.2$ eV) generates valence band holes (h^+_{vb}) and conduction band electrons (e^-_{cb}). These electron–hole pairs can either recombine or interact separately with other molecules. The holes at the ZnO valence band can oxidize adsorbed water or hydroxide ions to produce hydroxyl radicals. Electrons in the conduction band can reduce molecular oxygen to superoxide anions ($O_2^{-\bullet}$) [21]. Produced hydroxyl radicals ($^\bullet OH_{ads}$) along with other oxidants, e.g., superoxide radical anion ($O_2^{-\bullet}$), can further mineralize organic compounds to end products (water and CO_2) (Eq. (1)).

$$\text{Organics} + (^\bullet OH_{ads}, O_2^{-\bullet}, \text{etc.}) \rightarrow \text{products} \quad (1)$$

The UV/ZnO technique depends on various parameters that can modify the degradation of organic matter present in aqueous samples, such as the ZnO concentration, pH, reaction time, illumination intensity, initial composition of the water and/or wastewaters and concentration of organic matter in the water and/or wastewaters.

However, the response obtained from a waste treatment method, results from the interactive influences of the different variables. When a combination of several independent variables and their interactions affect desired responses, response surface methodology (RSM) is an effective tool for optimizing the process [22]. RSM uses an experimental design such as the factorial design to fit a model by least squares technique. This technique provides a systematic way of working that allows conclusions to be drawn about the variables (or combinations of variables) that are most influential in the response factor [23].

Several researchers have studied the application of experimental design to the determination of influential variables in AOPs and their impacts in the degradation process [22,24–40]. However, it has never been applied to NP degradation. The aim of this report, therefore, is modeling of NP degradation by the UV–vis/ZnO process. Experimental design methodology was used to evaluate the influence of the ZnO loading rate, pH of reaction media, and initial concentration of NP on the NP removal rate constant in the water.

2. Experimental

2.1. Materials

Nonylphenol (NP) with purity of 99.5% was obtained from Dr. Ehrenstorfer-Schafers (Germany). ZnO, NaOH, H_2SO_4 were purchased from Merck (Germany) and used without further purification. Solutions were prepared by dissolving required quantity of NP in DDW before each experiment. For the photodegradation of NP, a solution containing known concentration of the NP and ZnO nanopowder was prepared and it was allowed to equilibrate for 30 min in the darkness, then 1 L of the prepared suspension was transferred to the reactor, then the lamp was switched on to initiate the reaction.

2.2. Photocatalytic reaction system

Photo-oxidation of nonylphenol was conducted in an annular cylindrical batch reactor with a double layer quartz sleeve at the

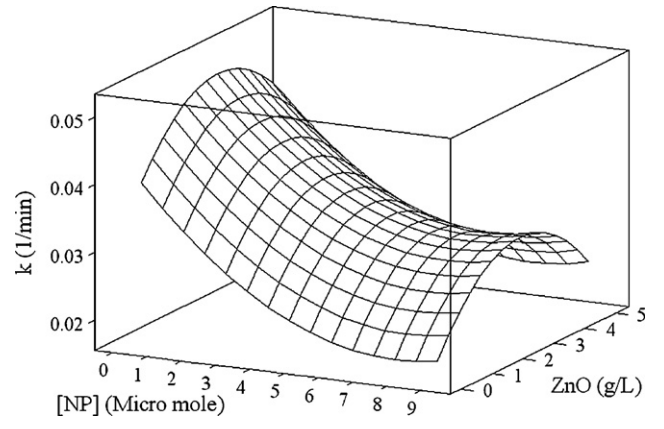

Fig. 2. The response surface plot of the NP degradation rate constant as the function of initial NP concentration (μM) and ZnO loading rate ($g\,L^{-1}$).

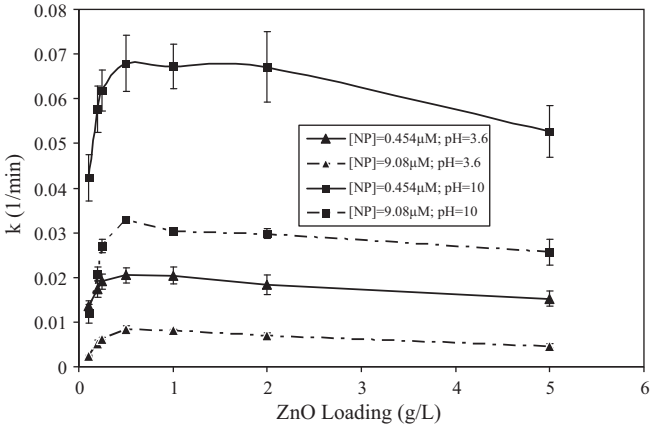

Fig. 4. Effects of ZnO loading on the photocatalytic degradation of NP.

Table 1
Design matrix and results obtained for samples (ZnO loading = 0.1–0.5 g L^{-1}).

Assays	[ZnO] (g L^{-1})	[NP] (μM)	pH	k (min^{-1})	Assays	[ZnO] (g L^{-1})	[NP] (μM)	pH	k (min^{-1})
1	0.1	0.454	3.6	0.01365	41	0.25	0.454	3.6	0.02249
2	0.1	0.454	6.2	0.02556	42	0.25	0.454	6.2	0.04059
3	0.1	0.454	7.5	0.03052	43	0.25	0.454	7.5	0.05250
4	0.1	0.454	8.7	0.03807	44	0.25	0.454	8.7	0.05929
5	0.1	0.454	10	0.04226	45	0.25	0.454	10	0.07269
6	0.1	2.27	3.6	0.00608	46	0.25	2.27	3.6	0.01390
7	0.1	2.27	6.2	0.01271	47	0.25	2.27	6.2	0.02899
8	0.1	2.27	7.5	0.01519	48	0.25	2.27	7.5	0.03089
9	0.1	2.27	8.7	0.01684	49	0.25	2.27	8.7	0.03620
10	0.1	2.27	10	0.02379	50	0.25	2.27	10	0.04399
11	0.1	4.54	3.6	0.00381	51	0.25	4.54	3.6	0.00947
12	0.1	4.54	6.2	0.01020	52	0.25	4.54	6.2	0.02095
13	0.1	4.54	7.5	0.01174	53	0.25	4.54	7.5	0.02442
14	0.1	4.54	8.7	0.01300	54	0.25	4.54	8.7	0.02797
15	0.1	4.54	10	0.01738	55	0.25	4.54	10	0.03574
16	0.1	9.08	3.6	0.00243	56	0.25	9.08	3.6	0.00626
17	0.1	9.08	6.2	0.00814	57	0.25	9.08	6.2	0.01518
18	0.1	9.08	7.5	0.00791	58	0.25	9.08	7.5	0.01848
19	0.1	9.08	8.7	0.00987	59	0.25	9.08	8.7	0.02160
20	0.1	9.08	10	0.01187	60	0.25	9.08	10	0.02701
21	0.2	0.454	3.6	0.02037	61	0.5	0.454	3.6	0.02046
22	0.2	0.454	6.2	0.03708	62	0.5	0.454	6.2	0.03827
23	0.2	0.454	7.5	0.04780	63	0.5	0.454	7.5	0.04803
24	0.2	0.454	8.7	0.05425	64	0.5	0.454	8.7	0.05231
25	0.2	0.454	10	0.06789	65	0.5	0.454	10	0.06793
26	0.2	2.27	3.6	0.00989	66	0.5	2.27	3.6	0.01495
27	0.2	2.27	6.2	0.01800	67	0.5	2.27	6.2	0.03145
28	0.2	2.27	7.5	0.02414	68	0.5	2.27	7.5	0.03342
29	0.2	2.27	8.7	0.02719	69	0.5	2.27	8.7	0.03838
30	0.2	2.27	10	0.03471	70	0.5	2.27	10	0.04678
31	0.2	4.54	3.6	0.00701	71	0.5	4.54	3.6	0.01102
32	0.2	4.54	6.2	0.01405	72	0.5	4.54	6.2	0.02577
33	0.2	4.54	7.5	0.02101	73	0.5	4.54	7.5	0.02905
34	0.2	4.54	8.7	0.02347	74	0.5	4.54	8.7	0.03129
35	0.2	4.54	10	0.02865	75	0.5	4.54	10	0.04159
36	0.2	9.08	3.6	0.00511	76	0.5	9.08	3.6	0.00840
37	0.2	9.08	6.2	0.01038	77	0.5	9.08	6.2	0.02224
38	0.2	9.08	7.5	0.01457	78	0.5	9.08	7.5	0.02370
39	0.2	9.08	8.7	0.01757	79	0.5	9.08	8.7	0.02735
40	0.2	9.08	10	0.02084	80	0.5	9.08	10	0.03284

center of the reactor to house a UV–vis light source. Experiments were conducted with 1 L suspension of ZnO and nonylphenol (Labor Dr. Ehrenstorfer-Schafers, Germany) in DDW. A magnetic stirrer was used to induce satisfactory mixing of the solution in the reactor. The temperature of the system was maintained at 26 (±0.5) °C by a quartz cooling water jacket surrounding the quartz sleeve. Depending on the degradation rates under individual reaction conditions, aliquots were sampled and ZnO was separated from suspensions using a centrifuge prior to analysis. Total volume of the withdrawn sample was less than 2% (by volume) of the solution. To investigate pH effects, pH of the reaction media was adjusted using H_2SO_4 and NaOH to a desired value throughout the experiments. Temperature and pH (using Metrohm 744 pH-meter, Switzerland) of reaction media were measured throughout each experiment. Nonporous ZnO (Merck, Germany) with primary particle diameter of 43 nm was used as the catalyst. Illumination was performed with UV–vis medium pressure mercury lamp (125 W, λ_{max} = 360 nm), which was placed in central of the quartz sleeve. The UV–vis light intensity in the vicinity of the bulk solution was measured at the external quartz sheath surface and internal reactor surface using a digital UVA radiometer (model EC1 UV-A, Hagner, Bosham, UK). The average intensity of illumination at $\lambda > 300$ nm was 9.3 mW cm^{-2}.

2.3. Chemical analysis

Nonylphenol was analyzed using a Shimadzu 10Avp Series high performance liquid chromatography system (Shimadzu, Japan) coupled with a RF-10A_{XL} programmable fluoresces detector. HPLC separations were performed using a Kromasil 100 C18 column (4.6 mm × 150 mm, 5 μm) from Eka Chemicals AB (Bohus, Sweden) thermostatted at 40 °C, injection volumes of 20 μL, flow rate of 2 mL min^{-1} and isocratic elution with 40% water and 60% acetonitrile during 25 min. Analytes were monitored by fluorescence detection (λ_{ex}: 222 nm, λ_{em}: 305 nm) and quantified by external calibration using peak area measurements. The extent of NP mineralization was determined through TOC analysis using a Shimadzu model TOC-V_{CSH} analyzer (Shimadzu, Japan).

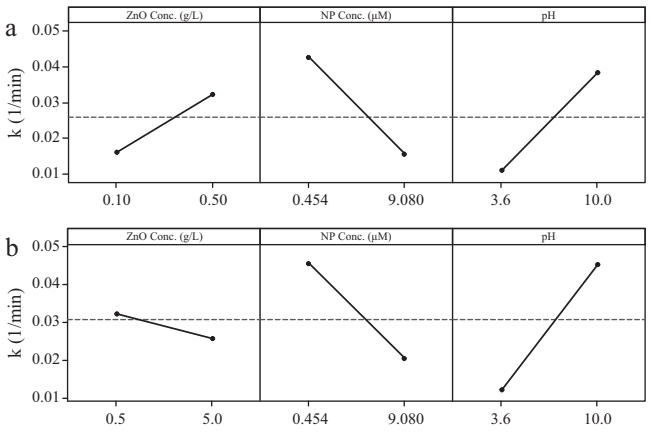

Fig. 5. Main Effects Plot for NP degradation rate coefficient (k (L min^{-1})). ZnO loading rate 0.1–0.5 g L^{-1} (b) ZnO loading rate 0.5–5.0 g L^{-1}.

Table 2
Design matrix and results obtained for samples (ZnO loading = 0.5-5.0 g L^{-1}).

Assays	[ZnO] (g L^{-1})	[NP] (μM)	pH	k (min^{-1})	Assays	[ZnO] (g L^{-1})	[NP] (μM)	pH	k (min^{-1})
1	0.5	0.454	3.6	0.02046	41	2.0	0.454	3.6	0.01987
2	0.5	0.454	6.2	0.03827	42	2.0	0.454	6.2	0.04144
3	0.5	0.454	7.5	0.04803	43	2.0	0.454	7.5	0.05179
4	0.5	0.454	8.7	0.05231	44	2.0	0.454	8.7	0.05866
5	0.5	0.454	10	0.06793	45	2.0	0.454	10	0.07251
6	0.5	2.27	3.6	0.01495	46	2.0	2.27	3.6	0.01390
7	0.5	2.27	6.2	0.03145	47	2.0	2.27	6.2	0.02737
8	0.5	2.27	7.5	0.03342	48	2.0	2.27	7.5	0.02979
9	0.5	2.27	8.7	0.03838	49	2.0	2.27	8.7	0.03560
10	0.5	2.27	10	0.04678	50	2.0	2.27	10	0.04488
11	0.5	4.54	3.6	0.01102	51	2.0	4.54	3.6	0.00995
12	0.5	4.54	6.2	0.02577	52	2.0	4.54	6.2	0.02660
13	0.5	4.54	7.5	0.02905	53	2.0	4.54	7.5	0.02962
14	0.5	4.54	8.7	0.03129	54	2.0	4.54	8.7	0.03443
15	0.5	4.54	10	0.04159	55	2.0	4.54	10	0.04127
16	0.5	9.08	3.6	0.00840	56	2.0	9.08	3.6	0.00705
17	0.5	9.08	6.2	0.02224	57	2.0	9.08	6.2	0.02018
18	0.5	9.08	7.5	0.02370	58	2.0	9.08	7.5	0.02162
19	0.5	9.08	8.7	0.02735	59	2.0	9.08	8.7	0.02543
20	0.5	9.08	10	0.03284	60	2.0	9.08	10	0.02979
21	1.0	0.454	3.6	0.02241	61	5.0	0.454	3.6	0.01524
22	1.0	0.454	6.2	0.04231	62	5.0	0.454	6.2	0.03333
23	1.0	0.454	7.5	0.05276	63	5.0	0.454	7.5	0.04136
24	1.0	0.454	8.7	0.06111	64	5.0	0.454	8.7	0.04404
25	1.0	0.454	10	0.07389	65	5.0	0.454	10	0.05263
26	1.0	2.27	3.6	0.01509	66	5.0	2.27	3.6	0.00931
27	1.0	2.27	6.2	0.02983	67	5.0	2.27	6.2	0.02381
28	1.0	2.27	7.5	0.03205	68	5.0	2.27	7.5	0.02532
29	1.0	2.27	8.7	0.03877	69	5.0	2.27	8.7	0.02950
30	1.0	2.27	10	0.04804	70	5.0	2.27	10	0.03862
31	1.0	4.54	3.6	0.01092	71	5.0	4.54	3.6	0.00753
32	1.0	4.54	6.2	0.02713	72	5.0	4.54	6.2	0.02310
33	1.0	4.54	7.5	0.02977	73	5.0	4.54	7.5	0.02540
34	1.0	4.54	8.7	0.03552	74	5.0	4.54	8.7	0.02808
35	1.0	4.54	10	0.04255	75	5.0	4.54	10	0.03384
36	1.0	9.08	3.6	0.00808	76	5.0	9.08	3.6	0.00468
37	1.0	9.08	6.2	0.02057	77	5.0	9.08	6.2	0.01578
38	1.0	9.08	7.5	0.02271	78	5.0	9.08	7.5	0.01845
39	1.0	9.08	8.7	0.02590	79	5.0	9.08	8.7	0.02171
40	1.0	9.08	10	0.03037	80	5.0	9.08	10	0.02564

2.4. Experimental design

Multivariate analysis has become an important tool for obtaining valuable and statistically significant models of a phenomenon by performing a minimum set of well-chosen experiments. With a determined number of assays, information can be obtained regarding the importance of each variable and their interaction effects [41]. A full factorial design was selected, which this design is considered to be the most suitable when the study is directed towards modeling of a process. The computer program used was the Windows version of MINITAB®. This is a statistical software package for the design of experiments and obtaining graphs, statistical parameters and modeling a process. The variables considered for this study were: ZnO loading rate, pH of reaction media, and initial concentration of NP. The variables and the values are as follow:

ZnO loading rate: 0.1, 0.2, 0.25, 0.5, 1, 2, and 5 g L^{-1}.
pH: 3.6, 6.2, 7.5, 8.7, and 10.
NP concentration: 0.454, 2.27, 4.54, and 9.08 μM.
Reaction time: 120 min.

A total of 140 experiments with 120 min reaction time were carried out in triplicate.

3. Results and discussion

3.1. RSM plots

The NP degradation rate constant response surface graphs are shown in Figs. 1–3. Fig. 1 illustrates the effect of initial NP concentration and pH on NP degradation constant for ZnO loading rate and reaction time of 0.1–5.0 g L^{-1} and 120 min, respectively. As it is obvious from Fig. 1, NP degradation efficiency decreased with increasing initial NP concentration. At a higher initial NP concentration, two factors could impede the degradation of NP; at first, increased amount of NP may cover a greater number of ZnO active sites, which afterwards suppresses generation of the oxidants and results in lower degradation rate constants. Secondly, a higher NP concentration absorbs more photons, consequently decreasing available photons to activate ZnO. Thus, an insufficiency of photons to activate ZnO surface basically retarded the degradation of NP at a high initial concentration. Hence, the overall reaction rates were lowered with the higher initial NP concentration. As is also evident from the Fig. 1, increasing the medium pH from 3.6 up to 10 increased NP degradation rate constant. This can be attributed to enhanced formation of •OH, because at high pH (e.g., 10) more hydroxide ions available on ZnO surface can be easily oxidized and form more •OH, which consequently increases the efficiency of NP degradation. On the other hand, the reaction rate constant significantly decreased at pH 11.5, mainly due to surface ionization of

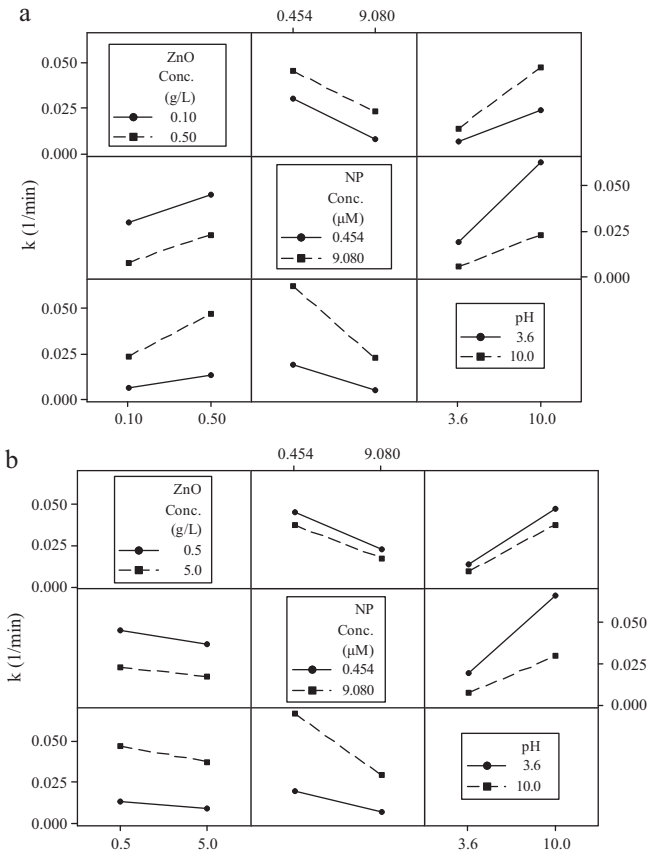

Fig. 6. Interaction Plot for NP degradation rate coefficient (k (L min^{-1})). (a) ZnO loading rate 0.1–0.5 g L^{-1} (b) ZnO loading rate 0.5–5.0 g L^{-1}.

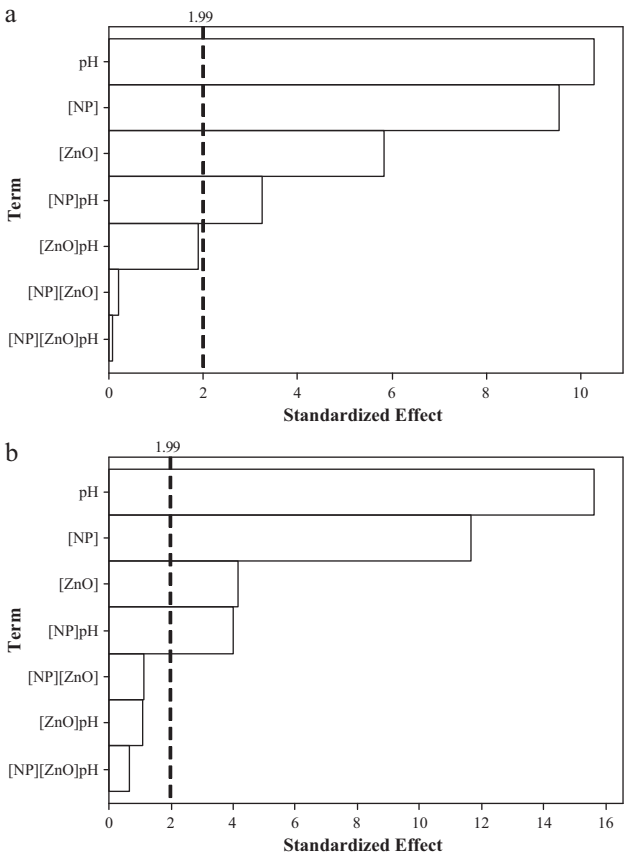

Fig. 7. Pareto chart of the standardized effects for NP degradation rate. (a) ZnO loading rate 0.1–0.5 g L^{-1} (b) ZnO loading rate 0.5–5.0 g L^{-1}. (response is k (L min^{-1}), Alpha = 0.05).

ZnO. Therefore, the optimum value of pH was obtained 10 in this study.

NP degradation rate constant obtained as a function of initial NP concentration and ZnO loading rate was depicted in Fig. 2. As it is clear from this figure, NP degradation rate constant increased with the increase of ZnO loading rate and reached a plateau at a ZnO loading of 0.5 g L^{-1}, and decreased slightly beyond 2.0 g L^{-1}. According to the Fig. 4 the curves are reminiscent of a Langmuir-type isotherm, suggesting that the k of the photo-oxidation reaches a saturation value at higher ZnO concentrations. This observation can be elucidated in terms of availability of active sites on the catalyst surface and the penetration of UV light into the suspension [31]. Additionally, at a larger catalyst loading, more of the originally activated ZnO may be deactivated through collision with ground-state catalysts [32]. Since agglomeration and sedimentation of ZnO under large catalyst loadings would also take place [33,34], available catalyst surface for photon absorption would definitely decrease, causing minor increase in the degradation rate beyond an optimum ZnO dosage, 0.5 g L^{-1} in this research.

Fig. 3 shows the response surface for NP degradation rate constant as a function of medium pH and ZnO loading rate at initial NP concentration of 0.454–9.08 μM. As can be seen from Fig. 3, the optimum values for medium pH and ZnO loading rate were 10 and 0.5 g L^{-1}, respectively.

3.2. Experimental design

Tables 1 and 2 show the design matrixes obtained with the MINITAB computer program, which includes the conditions and results for each assay with respect to the response factor defined as reaction rate constant (k (min^{-1})). According to the effects of varying the ZnO loading rate on the observed reaction rate constant (k) of the NP degradation (Figs. 2–4), which shows that the degradation rate of NP increased with ZnO loading and reached a plateau at a ZnO loading of 0.5 g L^{-1}, and decreased slightly beyond 2.0 g L^{-1}, therefore, in order to obtain the best results of the model, the ZnO loading rate 0.1–5.0 g L^{-1} separate into two range as 0.1–0.5 and 0.5–5.0 g L^{-1} and two design matrixes were prepared.

Fig. 5 shows main effects plots (data means), representing the effect of each variable on the response factor. According to the Fig. 5, the effects of [NP] and pH of reaction media on the degradation of the NP in both range of ZnO loading rate is very similar in terms of negative and positive effects on response factor, respectively. Vice versa, the effect of ZnO loading rate on response factor is quite different in the two range of ZnO dosage. The degradation rate constant of NP decreased when the initial concentrations of NP increased from 0.454 to 9.08 μM. However, increasing the pH of reaction media produces a higher degree of degradation. The ZnO loading rate has both positive and negative effects in ZnO dosage ranges of 0.1–0.5 and 0.5–5.0 g L^{-1}, respectively. This observation can be elucidated in terms of availability of active sites on the catalyst surface and the penetration of UV light into the suspension [42]. Additionally, at a larger catalyst loading, more of the originally activated ZnO may be deactivated through collision with ground-state catalysts [43]. Since agglomeration and sedimentation of ZnO under large catalyst loadings would also take place [44,45], available catalyst surface for photon absorption would definitely decrease, causing minor increase in the degradation rate beyond an optimum ZnO dosage, 0.5 g L^{-1} in this research. In Fig. 5, the slope of the plot is elucidative of the significance of the variable, and it can thus be seen that the NP concentration and pH of

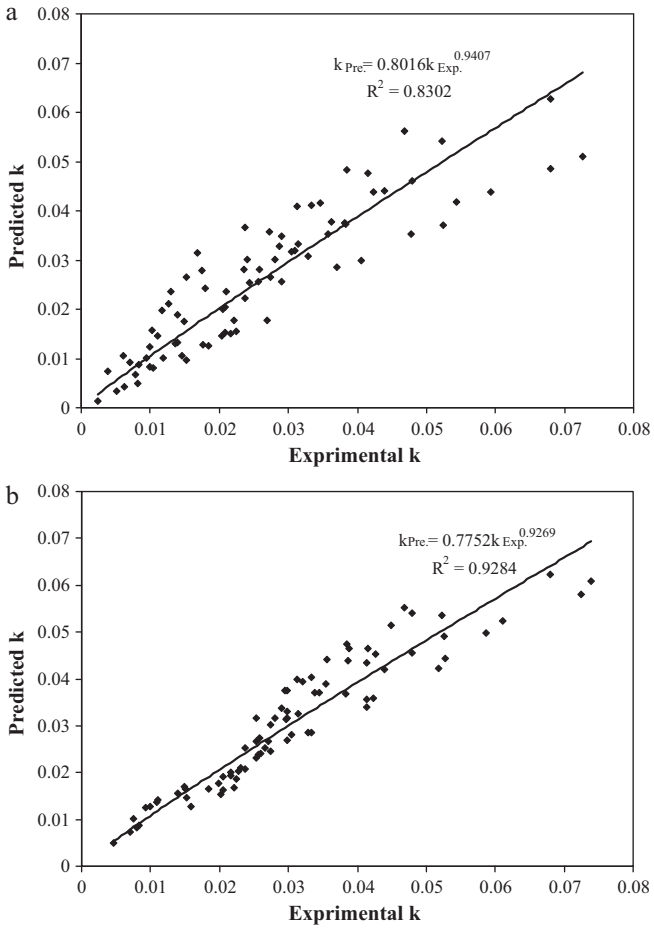

Fig. 8. Comparison between experimental and predicted rate constants for the photocatalytic oxidation of NP, (a) ZnO loading rate 0.1–0.5 g L^{-1} (b) ZnO loading rate 0.5–5.0 g L^{-1}.

reaction media are very influential variables while the ZnO loading rate is much less important for the confidence level selected.

Fig. 6 demonstrates full interaction plots showing the existence or otherwise of interaction among the variables. An interaction between variables occurs when the change in response from the low level to the high level of one variable is not the same as the change in response at the same two levels of a second variable. That is, the effect of one variable is dependent upon a second variable. Parallel or almost parallel plots in Fig. 6 represent that the interaction between the variables is not significant, whereas plots which are crossed or tending to cross show a significant interaction between the variables in question. As Fig. 6 indicates, the most significant interaction is: [NP]-pH ($p_{value} < 0.05$). According to the results, for low NP concentrations, the pH of reaction media has more influence in increasing of the response factor.

Eventually, a Pareto chart is used to draw conclusions as which of these variables and interactions are most significant. The MINITAB® statistical analysis program uses Lenth's method [24] in the case of factorial designs. This chart shows both the magnitude and the importance of the effects (variables or interactions). It exhibits the all variables and their iteractions in the ordinate and the pseudo-error standard of the effects in the abscissa. The study is done for a 95% confidence interval. On the Pareto chart there is a reference line (the discontinuous vertical plot), and any effect that extends past this line is potentially important. The reference line corresponds to a simultaneous margin of error. Pareto charts are shown in Fig. 7a and b (ZnO loading rate 0.1–0.5 g L^{-1} and ZnO loading rate 0.5–5.0 g L^{-1}). The variables and interactions which can be considered as especially important for the treatment of NP samples by UV–vis/ZnO treatment are: pH of reaction media, NP concentration, ZnO loading rate, [NP] × pH interaction.

The reduced models have been obtained taking into account the most significant variables and their interactions (pH of reaction media, NP concentration and ZnO loading rate and the [NP] × pH interaction) in this photocatalysis process. For the treatment of NP samples with ZnO loading rate 0.1–0.5 g L^{-1}, the reduced model that describes the degradation process is governed by the following Eq. (2):

$$k = 0.02384 + 0.00678[\mathrm{ZnO}] - 0.01105[\mathrm{NP}] + 0.01305\mathrm{pH} - 0.00539[\mathrm{NP}] \times \mathrm{pH} \quad (2)$$

In the case of ZnO loading rate 0.5–5.0 g L^{-1}, the following equation applies (3):

$$k = 0.02643 - 0.00329[\mathrm{ZnO}] - 0.009914[\mathrm{NP}] + 0.01456\mathrm{pH} - 0.00486[\mathrm{NP}] \times \mathrm{pH} \quad (3)$$

Fig. 8 shows the experimental rate constants values obtained in each experiment (Tables 1 and 2) vs. the predicted values for the NP degradation rate constant calculated by proposed models. It can be observed that the predicted k has good agreement with the experimental k (R^2 = 0.83 and 0.93 with ZnO loading range 0.1–0.5 and 0.5–5.0 g L^{-1}, respectively). Comparison between calculated and experimental values of the response variable of NP degradation was evaluated by linear equations. The values of R^2 were found to be 0.80 and 0.89, with ZnO loading range 0.1–0.5 and 0.5–5.0 g L^{-1}, respectively. Results confirm that the experimental values are in best fit with the predicted values according to the exponential equations.

In spite of the satisfactory results obtained with the reduced models, it is important to emphasis that this research work is a preliminary study addressed mainly towards gaining knowledge of the influential variables in the UV–vis/ZnO process applied to treatment of NP. The models can satisfactorily describe the photocatalysis technology in homogeneous phase as applied to such treatment.

4. Conclusions

This work shows that NP can be degraded by UV–vis/ZnO process. Effect of experimental parameters on the degradation efficiency of NP was established by the response surface plots of the response factor (k). Experimental results showed that the NP degradation rate constants decrease with an increase in the initial concentration of NP, but increased with larger ZnO loading and reached a plateau at ZnO concentration of 0.5 g L^{-1} and decreased slightly at a very high concentration of 5.0 g L^{-1}. The rate constant increases with increase in pH up to 10, after which a significant decrease is observed. The influence of each variable and of their interactions with respect to the response factor has been studied by means of a full factorial design with three replicates. The most important variables and interactions in the process and empirical models that describe degradation process have been established. It is observed that the degree of NP removal depends mainly on the initial NP concentration, ZnO dosages and pH of reaction media and [NP] × pH interaction, while all other interactions variables were not significant in this study and each variable influence the response factor (k) independently. The reduced empirical models were chosen on the basis of the significant variables and interactions obtained in the Pareto chart. It is demonstrated that the models can be used to predict the reaction rate constant of this treatment.

Acknowledgements

The authors would like to thank the Research Deputy of Tehran University of Medical Sciences for financial support. We gratefully acknowledge Pharmacy Faculty of Jondishapour University of Medical Sciences for their technical assistance.

References

[1] M. Fountoulakis, P. Drillia, C. Pakou, A. Kampioti, K. Stamatelatou, G. Lyberatos, Analysis of nonylphenol and nonylphenol ethoxylates in sewage sludge by high performance liquid chromatography following microwave-assisted extraction, J. Chromatogr. A 1089 (2005) 45–51.
[2] M. Ahel, W. Giger, M. Koch, Behaviour of alkylphenol polyethoxylate surfactants in the aquatic environment-I. Occurrence and transformation in sewage treatment, Water Res. 28 (1994) 1131–1142.
[3] M. Ahel, W. Giger, C. Schaffner, Behaviour of alkylphenol polyethoxylate surfactants in the aquatic environment-II. Occurrence and transformation in rivers, Water Res. 28 (1994) 1143–1152.
[4] M.A. Blackburn, M.J. Waldock, Concentrations of alkylphenols in rivers and estuarines in England and Wales, Water Res. 29 (1995) 1623–1629.
[5] K. Inumaru, M. Murashima, T. Kasahara, S. Yamanaka, Enhanced photocatalytic decomposition of 4-nonylphenol by surface-organografted TiO_2: a combination of molecular selective adsorption and photocatalysis, Appl. Catal. B: Environ. 52 (2004) 275–280.
[6] USEPA Testing consent order on 4-nonylphenol, branched, Fed Reg 35 (1990) 5991–5994.
[7] L. Brooke, G. Thursby, Ambient aquatic life water quality criteria for nonylphenol., Washington DC, USA: Report for the United States EPA, Office of Water, Office of Science and Technology (2005).
[8] J. Kim, G.V. Korshin, A.B. Velichenko, Comparative study of electrochemical degradation and ozonation of nonylphenol, Water Res. 39 (2005) 2527–2534.
[9] K. Lenz, V. Beck, M. Fuerhacker, Behaviour of bisphenol A (BPA), 4-nonylphenol (4-NP) and 4-nonylphenol ethoxylates (4-NP1EO, 4-NP2EO) in oxidative water treatment water processes, Water Sci. Technol. 50 (2004) 141–147.
[10] B. Ning, N.J.D. Graham, Y. Zhang, Degradation of octylphenol and nonylphenol by ozone – Part I: direct reaction, Chemosphere 68 (2007) 1163–1172.
[11] B. Ning, N.J.D. Graham, Y. Zhang, Degradation of octylphenol and nonylphenol by ozone – Part II: indirect reaction, Chemosphere 68 (2007) 1173–1179.
[12] M. Ike, M. Asano, F.D. Belkada, S. Tsunoi, M. Tanaka, M. Fujita, Degradation of biotansformation products of nonylphenol ethoxylates by ozonation and UV/TiO_2 treatment, Water Sci. Technol. 46 (2002) 127–132.
[13] M. Neamtu, F.H. Frimmel, Photodegradation of endocrine disrupting chemical nonylphenol by simulated solar UV-irradiation, Sci. Total Environ. 369 (2006) 295–306.
[14] S. Kohtani, J. Hiro, N. Yamamoto, A. Kudo, K. Tokumura, R. Nakagaki, Adsorptive and photocatalytic properties of Ag-loaded BiVO4 on the degradation of 4-n-alkylphenols under visible light irradiation, Catal. Commun. 6 (2005) 185–189.
[15] E. Pelizzetti, C. Minero, V. Maurino, A. Sclafani, H. Hidaka, N. Serpone, Photocatalytic degradation of nonylphenol ethoxylated surfactants, Environ. Sci. Technol. 23 (1989) 1380–1385.
[16] S. Kohtani, M. Koshiko, A. Kudo, K. Tokumura, Y. Ishigaki, A. Toriba, K. Hayakawa, R. Nakagaki, Photodegradation of 4-alkylphenols using BiVO4 photocatalyst under irradiation with visible light from a solar simulator, Appl. Catal. B: Environ. 46 (2003) 573–586.
[17] B. Yim, Y. Yoo, Y. Maeda, Sonolysis of alkylphenols in aqueous solution with Fe(II) and Fe(III), Chemosphere 50 (2003) 1015–1023.
[18] A. Eslami, S. Nasseri, B. Yadollahi, A. Mesdaghinia, F. Vaezi, R. Nabizadeh, S. Nazmara, Photocatalytic degradation of methyl tert-butyl ether (MTBE) in contaminated water by ZnO nanoparticles, J. Chem. Technol. Biotechnol. 83 (2008) 1447–1453.
[19] M.R. Hoffmann, S.T. Martin, W. Choi, D.W. Bahnemann, Environmental applications of semiconductor photocatalysis, Chem. Rev. 95 (1995) 69–96.
[20] A. Mills, S. Le Hunte, An overview of semiconductor photocatalysis, J. Photochem. Photobiol. A: Chem. 108 (1997) 1–35.
[21] M.A. Behnajady, N. Modirshahla, N. Daneshvar, M. Rabbani, Photocatalytic degradation of C.I. Acid Red 27 by immobilized ZnO on glass plates in continuous-mode, J. Hazard. Mater. 140 (2007) 257–263.
[22] M. Ahmadi, A. Mesdaghinia, K. Naddfi, R. Nabizadeh, S. Nasseri, A.H. Mahvi, F. vaezi, Modeling of 2,4dinitrophenol degradation by modified-fenton process via multivariate approach, Res. J. Chem. Environ. 13 (2009) 19–23.
[23] D.C. Montgomery, Design and Analysis of Experiments, Willey, New York, 2001.
[24] M.P. Ormad, R. Mosteo, C. Ibarz, J.L. Ovelleiro, Multivariate approach to the photo-Fenton process applied to the degradation of winery wastewaters, Appl. Catal. B: Environ. 66 (2006) 58–63.
[25] J. Fernandez, J. Kiwi, C. Lizama, J. Freer, J. Baeza, H.D. Mansilla, Factorial experimental design of Orange II photocatalytic discolouration, J. Photochem. Photobiol. A: Chem. 151 (2002) 213–219.
[26] M. Pérez, F. Torrades, J. Peral, C. Lizama, C. Bravo, S. Casas, J. Freer, H.D. Mansilla, Multivariate approach to photocatalytic degradation of a cellulose bleaching effluent, Appl. Catal. B: Environ. 33 (2001) 89–96.
[27] J.H. Ramirez, C.A. Costa, L.M. Madeira, Experimental design to optimize the degradation of the synthetic dye Orange II using Fenton's reagent, Catal. Today 107–108 (2005) 68–76.
[28] J. Fernandez, J. Kiwi, J. Baeza, J. Freer, C. Lizama, H.D. Mansilla, Orange II photocatalysis on immobilised TiO_2: Effect of the pH and H_2O_2, Appl. Catal. B: Environ. 48 (2004) 205–211.
[29] H. Zhang, H.J. Choi, P. Canazo, C.-P. Huang, Multivariate approach to the Fenton process for the treatment of landfill leachate, J. Hazard. Mater. 161 (2009) 1306–1312.
[30] W.C. Paterlini, R.F.P. Nogueira, Multivariate analysis of photo-Fenton degradation of the herbicides tebuthiuron, diuron and 2,4-D, Chemosphere 58 (2005) 1107–1116.
[31] A.G. Trovo, W.C. Paterlini, R.F.P. Nogueira, Evaluation of the influences of solution path length and additives concentrations on the solar photo-Fenton degradation of 4-chlorophenol using multivariate analysis, J. Hazard. Mater. 137 (2006) 1577–1582.
[32] C.S.D. Rodrigues, L.M. Madeira, R.A.R. Boaventura, Optimization of the azo dye Procion Red H-EXL degradation by Fenton's reagent using experimental design, J. Hazard. Mater. 164 (2009) 987–994.
[33] R. Mosteo, P.a. Ormad, E. Mozas, J. Sarasa, J.L. Ovelleiro, Factorial experimental design of winery wastewaters treatment by heterogeneous photo-Fenton process, Water Res. 40 (2006) 1561–1568.
[34] F. Torrades, M. Pérez, H.D. Mansilla, J. Peral, Experimental design of Fenton and photo-Fenton reactions for the treatment of cellulose bleaching effluents, Chemosphere 53 (2003) 1211–1220.
[35] P. Calza, V.A. Sakkas, A. Villioti, C. Massolino, V. Boti, E. Pelizzetti, T. Albanis, Multivariate experimental design for the photocatalytic degradation of imipramine: determination of the reaction pathway and identification of intermediate products, Appl. Catal. B: Environ. 84 (2008) 379–388.
[36] P. Durango-Usuga, F. Guzman-Duque, R. Mosteo, M.V. Vazquez, G. Penuela, R.A. Torres-Palma, Experimental design approach applied to the elimination of crystal violet in water by electrocoagulation with Fe or Al electrodes, J. Hazard. Mater. 179 (2010) 120–126.
[37] I. Grcic, M. Muzic, D. Vujevic, N. Koprivanac, Evaluation of atrazine degradation in UV/FeZSM-5/H_2O_2 system using factorial experimental design, Chem. Eng. J. 150 (2009) 476–484.
[38] P. Kralik, H. Kusic, N. Koprivanac, A. Loncaric, A.L. Bozic, Degradation of chlorinated hydrocarbons by UV/H_2O_2: The application of experimental design and kinetic modeling approach, Chem. Eng. J. 158 (2010) 154–166.
[39] C. Fernandez, M.S. Larrechi, M.P. Callao, Study of the influential factors in the simultaneous photocatalytic degradation process of three textile dyes, Talanta 79 (2009) 1292–1297.
[40] R. Oliveira, M.F. Almeida, L.c. Santos, L.M. Madeira, Experimental design of 2,4-dichlorophenol oxidation by Fenton's reaction, Ind. Eng. Chem. Res. 45 (2006) 1266–1276.
[41] M. Peĭrez, F. Torrades, J. Peral, C. Lizama, C. Bravo, S. Casas, J. Freer, H. Mansilla, Multivariate approach to photo catalytic degradation of cellulose bleaching effluent, Appl. Catal. B Environ. 33 (2001) 89–96.
[42] N. Daneshvar, M. Rabbani, N. Modirshahla, M.A. Behnajady, Kinetic modeling of photocatalytic degradation of Acid Red 27 in UV/TiO_2 process, J. Photochem. Photobiol. A: Chem. 168 (2004) 39–45.
[43] B. Neppolian, H.C. Choi, S. Sakthivel, B. Arabindoo, V. Murugesan, Solar/UV-induced photocatalytic degradation of three commercial textile dyes, J. Hazard. Mater. 89 (2002) 303–317.
[44] C.M. So, M.Y. Cheng, J.C. Yu, P.K. Wong, Degradation of azo dye Procion Red MX-5B by photocatalytic oxidation, Chemosphere 46 (2002) 905–912.
[45] N. San, M. Kılıç, Z. Çınar, Enhancement and Modeling of the Photocatalytic Degradation of Benzoic Acid, J. Adv. Oxid. Technol. 10 (2007) 51–59.